City Research Online

City, University of London Institutional Repository

This is the accepted version of the paper.

This version of the publication may differ from the final published version.

General Unbiased FIR Filter With Applications to GPS-Based Steering of Oscillator Frequency

Yuriy S. Shmaliy, Sanowar H. Khan, Shunyi Zhao, and Oscar Ibarra-Manzano

Abstract— The general unbiased finite-impulse response (UFIR) filter proposed in this brief has important structural advantages against its basic predecessor. It can be applied to systems with or without the control input. We derive this filter in a batch form and then design its fast iterative Kalman-like algorithm using recursions. The iterative UFIR algorithm proposed is applied to the three-state polynomial model which is basic in clock synchronization. We test it by the global positioning system-based frequency steering of an oven-controlled crystal oscillator. Better robustness and higher accuracy of the UFIR filter against the Kalman filter are shown experimentally.

Index Terms— Control system, global positioning system (GPS)-based frequency steering, Kalman filter (KF), state space, unbiased finite-impulse response (UFIR) filter, unbiasedness.

I. INTRODUCTION

ACCURATE signal estimation and control of diverse electronic systems are required in discrete time if control units are equipped with digital signal processing (DSP) blocks. Many problems associated with control [1], localization [2], position and velocity estimation [3], tracking [4], [5], and digital communications [6] are efficiently solved using DSP. For example, the global positioning system (GPS) one pulse per second (1PPS) timing signals [7] are used to discipline frequency of local oscillators, thereby providing sources of precise and accurate time and frequency [8], which are cheap and available for any purpose [9] in application [10].

Because many electronic systems operate in real time, fast optimal estimators are required. A traditional tool here is the recursive Kalman filter (KF) [11] and its modifications [12]. An annoying specific of real-world operation is that it often implies different kinds of uncertainties, mismodeling, and artificial interferences in unknown or not fully known noise environments. An estimator must thus be sufficiently robust.

But what many issues are facing in practice of the KF use says the opposite. The KF holds the following.

1) It has low robustness against mismodeling and temporary uncertainties [13] that may cause divergence when a system is nonlinear [14].
2) It is sensitive to errors in the imprecisely defined noise statistics [15] that may also lead to divergence in non-linear cases [16].
3) It requires initial state and initial error statistics [17] that cannot always be provided.

Analyzing these issues, Jazwinski [18] concluded that the low performance of KF in real world has a lot to do with its infinite impulse response. He then summarized in [19] that a limited memory filter appears to be the only device for preventing divergence in the presence of unbounded perturbation in the system. Since the limited memory transversal filter has the finite-impulse response (FIR), it also has the bounded input/bounded output stability, not peculiar to KF, and produces smaller round-off errors [20], [21].

Later, many researchers came up with a conclusion that the FIR filter is more robust than the KF [10], [13], [15], [22]–[25]. But the FIR filter is a batch estimator and its convolution-based structure is often inappropriate for real-time estimation. Therefore, efforts were made to find fast algorithms similar to recursive Gauss's ordinarily least squares. Recursive forms for FIR filters were discussed in [21] and [26], a recursive limited memory filter was proposed in [27], a receding horizon Kalman FIR filter was designed in [28], a recursive algorithm for deterministic time-invariant control systems was developed in [29], a p-shift iterative unbiased FIR (UFIR) estimator was derived in [17], and iterative forms for optimal and bias-constrained FIR filters were recently found in [30] and [31].

Among possible fast Kalman-like FIR solutions, there is an iterative UFIR estimator [15], which completely ignores the noise statistics and does not require the initial state and initial error statistics. Like any other FIR filter, the UFIR one operates in discrete-time index n on a horizon of N neighboring points, from $n - N - 1$ to n. Its iterative form requires about $N - 1$ times more computation time than the KF and N must be set optimally, N_{opt}, in order to minimize the mean square error (mse). At a necessity to reduce the computation time, parallel computing can be organized.

It has to be remarked now that the iterative UFIR algorithm was derived in [15] for systems with no inputs. It is thus not adapted to closed-loop problems associated with control, synchronization, and adaptive filtering. Unlike the KF

incorporating the input via the prior estimate, the UFIR filter operates simultaneously with N points that needs more care in combining the state with the input.

In this brief, we derive and investigate a general batch UFIR filter and develop it to a fast iterative Kalman-like algorithm which can universally be applied to systems with or without the control inputs. The rest of the brief is organized as follows. In Section II, we describe the model. In Section III, we derive the general UFIR filter in a batch form and find its fast iterative Kalman-like algorithm. Applications to GPS-based frequency steering are given in Section IV, and the conclusions are drawn in Section V.

II. MODEL

Consider a general linear system represented in discrete-time index n with the state and observation equations, respectively

$$\mathbf{x}_n = \mathbf{F}_n\mathbf{x}_{n-1} + \mathbf{E}_n\mathbf{u}_n + \mathbf{D}_n\mathbf{w}_n \tag{1}$$

$$\mathbf{y}_n = \mathbf{H}_n\mathbf{x}_n + \mathbf{v}_n \tag{2}$$

where $\mathbf{x}_n \in \mathbb{R}^K$ is the state vector, $\mathbf{u}_n \in \mathbb{R}^L$ is the input signal vector, $\mathbf{y}_n \in \mathbb{R}^M$ is the state observation vector, and $\mathbf{F}_n \in \mathbb{R}^{K \times K}$, $\mathbf{D}_n \in \mathbb{R}^{K \times P}$, $\mathbf{H}_n \in \mathbb{R}^{M \times K}$, and $\mathbf{E}_n \in \mathbb{R}^{K \times L}$ are some known time-variant matrices. We suppose that the noise sources, $\mathbf{w}_n \in \mathbb{R}^P$ and $\mathbf{v}_n \in \mathbb{R}^M$, are zero mean, $E\{\mathbf{w}_n\} = \mathbf{0}$ and $E\{\mathbf{v}_n\} = \mathbf{0}$. To fit better practical cases when noise is not obligatorily white and Gaussian, we admit that $\mathbf{w}_n$ and $\mathbf{v}_n$ may have unspecified (arbitrary) distributions and covariances, $\mathbf{Q}(i, j) = E\{\mathbf{w}_i\mathbf{w}_j^T\}$ and $\mathbf{R}(i, j) = E\{\mathbf{v}_i\mathbf{v}_j^T\}$. We also suppose that $\mathbf{w}_n$ and $\mathbf{v}_n$ are mutually uncorrelated, $E\{\mathbf{w}_i\mathbf{v}_j^T\} = \mathbf{0}$, for all integers i and j.

A traditional approach in FIR filtering implies extending (1) and (2) on a horizon of N neighboring past points, from $m = n - N + 1$ to n, to represent system states on $[m, n]$ via the initial state $\mathbf{x}_m$. If to follow this rule [32], one may arrive at [17]:

$$\mathbf{X}_{m,n} = \mathbf{A}_{m,n}\mathbf{x}_m + \mathbf{S}_{m,n}\mathbf{U}_{m,n} + \mathbf{B}_{m,n}\mathbf{W}_{m,n} \tag{3}$$

$$\mathbf{Y}_{m,n} = \mathbf{C}_{m,n}\mathbf{x}_m + \mathbf{L}_{m,n}\mathbf{U}_{m,n} + \mathbf{G}_{m,n}\mathbf{W}_{m,n} + \mathbf{V}_{m,n} \tag{4}$$

where the extended vectors are $\mathbf{X}_{m,n} = [\mathbf{x}_m^T \ldots \mathbf{x}_n^T]^T$, $\mathbf{Y}_{m,n} = [\mathbf{y}_m^T \ldots \mathbf{y}_n^T]^T$, $\mathbf{U}_{m,n} = [\mathbf{u}_m^T \ldots \mathbf{u}_n^T]^T$, $\mathbf{W}_{m,n} = [\mathbf{w}_m^T \ldots \mathbf{w}_n^T]^T$, and $\mathbf{V}_{m,n} = [\mathbf{v}_m^T \ldots \mathbf{v}_n^T]^T$. The extended matrices are represented with

$$\mathbf{A}_{m,n} = \left[\mathbf{I} \ \mathbf{F}_{m+1}^T \ \ldots \ \left(\mathcal{F}_{n-1}^{m+1}\right)^T \ \left(\mathcal{F}_n^{m+1}\right)^T\right]^T \tag{5}$$

$$\mathbf{S}_{m,n} = \begin{bmatrix} \mathbf{E}_m & \mathbf{0} & \ldots & \mathbf{0} & \mathbf{0} \\ \mathbf{A}_{m+1}\mathbf{E}_m & \mathbf{E}_{m+1} & \ldots & \mathbf{0} & \mathbf{0} \\ \vdots & \vdots & \ddots & \vdots & \vdots \\ \mathcal{F}_{n-1}^{m+1}\mathbf{E}_m & \mathcal{F}_{n-1}^{m+2}\mathbf{E}_{m+1} & \ldots & \mathbf{E}_{n-1} & \mathbf{0} \\ \mathcal{F}_n^{m+1}\mathbf{E}_m & \mathcal{F}_n^{m+2}\mathbf{E}_{m+1} & \ldots & \mathbf{A}_n\mathbf{E}_{n-1} & \mathbf{E}_n \end{bmatrix} \tag{6}$$

$$\mathbf{C}_{m,n} = \bar{\mathbf{C}}_{m,n}\mathbf{A}_{m,n} \tag{7}$$

$$\mathbf{G}_{m,n} = \bar{\mathbf{C}}_{m,n}\mathbf{B}_{m,n} \tag{8}$$

$$\mathbf{L}_{m,n} = \bar{\mathbf{C}}_{m,n}\mathbf{S}_{m,n} \tag{9}$$

$$\bar{\mathbf{C}}_{m,n} = \mathrm{diag}(\underbrace{\mathbf{H}_m \ \mathbf{H}_{m+1} \ \ldots \ \mathbf{H}_n}_{N}) \tag{10}$$

$$\mathcal{F}_r^g = \begin{cases} \mathbf{F}_r\mathbf{F}_{r-1} \ldots \mathbf{F}_g, & g \leq r \\ \mathbf{I}, & g = r + 1 \\ \mathbf{0}, & \text{otherwise} \end{cases} \tag{11}$$

and matrix $\mathbf{B}_{m,n}$ can be written in the same form as (6) if to substitute $\mathbf{E}_i$ with $\mathbf{D}_i$, where $i \in [m, n]$. For more detail about this model, the reader is referred to [10] and [32].

Following [15], the FIR estimate $\hat{\mathbf{x}}_n$ of $\mathbf{x}_n$ can be defined in the discrete convolution-based batch form of:

$$\hat{\mathbf{x}}_n = \bar{\mathbf{H}}_{m,n}\mathbf{Y}_{m,n}$$
$$= \bar{\mathbf{H}}_{m,n}(\mathbf{C}_{m,n}\mathbf{x}_m + \mathbf{L}_{m,n}\mathbf{U}_{m,n} + \mathbf{G}_{m,n}\mathbf{W}_{m,n} + \mathbf{V}_{m,n}) \tag{12}$$

in which $\bar{\mathbf{H}}_{m,n}$ is known as the FIR filter gain [33], to be specified in some sense. Of practical importance is that $\bar{\mathbf{H}}_{m,n}$ found in the unbiased sense (unbiased gain) produces estimates very closely related to optimal $\bar{\mathbf{H}}_{m,n}$ minimizing the mse [17]. An important advantage of the unbiased gain is that it does not require any information about noise and initial values which are often unknown or not fully known in many applications.

III. UFIR FILTERING ESTIMATE

The UFIR filter satisfies the unbiasedness condition

$$E\{\hat{\mathbf{x}}_n\} = E\{\mathbf{x}_n\} \tag{13}$$

which means that the average of the estimate is guaranteed to be equal to that of the state, if the filter order is equal to that of the system. Condition (13) does not guarantee optimality. But what many real-world issues suggest is that tracking the mean value may be a better choice than optimal tracking in the uncertain noise environments. This is because errors in optimal estimators may be larger due to mismodeling and imprecisely defined noise statistics than errors in the unbiased estimator, which ignores the noise statistics and averages model errors.

To find $\bar{\mathbf{H}}_{m,n}$ obeying (13), we extract $\mathbf{x}_n$ as the first row vector from (3)

$$\mathbf{x}_n = \mathcal{F}_n^{m+1}\mathbf{x}_m + \mathbf{S}_{m,n}^{(N)}\mathbf{U}_{m,n} + \mathbf{B}_{m,n}^{(N)}\mathbf{W}_{m,n} \tag{14}$$

where $\mathbf{S}_{m,n}^{(N)}$ is the Nth vector rows of $\mathbf{S}_{m,n}$ given by (6)

$$\mathbf{S}_{m,n}^{(N)} = \left[\underbrace{\mathcal{F}_n^{m+1}\mathbf{E}_m \ \mathcal{F}_n^{m+2}\mathbf{E}_{m+1} \ \ldots \ \mathbf{A}_n\mathbf{E}_{n-1} \ \mathbf{E}_n}_{N} \right] \tag{15}$$

and $\mathbf{B}_{m,n}^{(N)}$ can be defined similar to $\mathbf{S}_{m,n}^{(N)}$ via $\mathbf{B}_{m,n}$.

By equating the average of $\hat{\mathbf{x}}_n$ given by (12) and the average of $\mathbf{x}_n$ given by (14), we arrive at an equation

$$(\bar{\mathbf{H}}_{m,n}\mathbf{C}_{m,n} - \mathcal{F}_n^{m+1})\mathbf{x}_m = (\mathbf{S}_{m,n}^{(N)} - \bar{\mathbf{H}}_{m,n}\mathbf{L}_{m,n})\mathbf{U}_{m,n} \tag{16}$$

which suggests the following. Because vectors $\mathbf{x}_m$ and $\mathbf{U}_{m,n}$ have different dimensions and physical sources, they generally cannot be equal to zero. Otherwise, we consider the case isolated when all of the components in $\mathbf{x}_m$ are zeros and all of the control signals $\mathbf{u}_n$ in extended vector $\mathbf{U}_{m,n}$ are also zeros on a horizon $[m, n]$. On the other hand, the terms in the parentheses of (16) cannot simultaneously be equal to zero in view of their mutual independence. That means that (16) can

be obeyed and the FIR filter will be unbiased if the following holds.

1) $\mathbf{U}_{m,n} = \mathbf{0}$ and $\bar{\mathbf{H}}_{m,n}^h \mathbf{C}_{m,n} = \mathcal{F}_n^{m+1}$ that corresponds to the homogenous solution with the homogenous gain $\bar{\mathbf{H}}_{m,n}^h$.

2) $\mathbf{x}_m = \mathbf{0}$ and $\mathbf{S}_{m,n}^{(N)} = \bar{\mathbf{H}}_{m,n}^f \mathbf{L}_{m,n}$ that corresponds to the forced solution with the forced gain $\bar{\mathbf{H}}_{m,n}^f$.

The first condition results in the unbiasedness constraint [20]

$$\bar{\mathbf{H}}_{m,n}^h \tilde{\mathbf{C}}_{m,n} = \mathbf{I} \tag{17}$$

if to assign $\tilde{\mathbf{C}}_{m,n} = \mathbf{C}_{m,n}(\mathcal{F}_n^{m+1})^{-1}$. From (17), we have the homogenous gain

$$\bar{\mathbf{H}}_{m,n}^h = (\tilde{\mathbf{C}}_{m,n}^T \tilde{\mathbf{C}}_{m,n})^{-1} \tilde{\mathbf{C}}_{m,n}^T \tag{18}$$

by substituting $\mathbf{I}$ with identity $(\tilde{\mathbf{C}}_{m,n}^T \tilde{\mathbf{C}}_{m,n})^{-1} \tilde{\mathbf{C}}_{m,n}^T \tilde{\mathbf{C}}_{m,n}$ and discarding the nonzero $\tilde{\mathbf{C}}_{m,n}$ from both sides.

Similarly, the second condition gives us the forced gain

$$\bar{\mathbf{H}}_{m,n}^f = \mathbf{S}_{m,n}^{(N)} (\mathbf{L}_{m,n}^T \mathbf{L}_{m,n})^{-1} \mathbf{L}_{m,n}^T. \tag{19}$$

Now, note that, by the definition, the homogenous gain $\bar{\mathbf{H}}_{m,n}^h$ (18) must be applied to observations with zero inputs which can be formed as $\mathbf{Y}_{m,n} - \mathbf{L}_{m,n}\mathbf{U}_{m,n}$. In turn, the forced gain $\bar{\mathbf{H}}_{m,n}^f$ (19) must be applied to the input signal $\mathbf{L}_{m,n}\mathbf{U}_{m,n}$, implying zero state. A superposition of the homogenous and forced solutions found in such a way leads to a general batch UFIR filter

$$\begin{aligned}
\hat{\mathbf{x}}_n &= \bar{\mathbf{H}}_{m,n}^h (\mathbf{Y}_{m,n} - \mathbf{L}_{m,n}\mathbf{U}_{m,n}) + \bar{\mathbf{H}}_{m,n}^f \mathbf{L}_{m,n}\mathbf{U}_{m,n} \\
&= \bar{\mathbf{H}}_{m,n}^h (\mathbf{Y}_{m,n} - \mathbf{L}_{m,n}\mathbf{U}_{m,n}) \\
&\quad + \mathbf{S}_{m,n}^{(N)} (\mathbf{L}_{m,n}^T \mathbf{L}_{m,n})^{-1} \mathbf{L}_{m,n}^T \mathbf{L}_{m,n}\mathbf{U}_{m,n} \\
&= \mathbf{S}_{m,n}^{(N)} \mathbf{U}_{m,n} + \bar{\mathbf{H}}_{m,n}^h (\mathbf{Y}_{m,n} - \mathbf{L}_{m,n}\mathbf{U}_{m,n}) \tag{20}
\end{aligned}$$

which can be applied to systems with inputs, $\mathbf{U}_{m,n} \neq \mathbf{0}$, or with no inputs, $\mathbf{U}_{m,n} = \mathbf{0}$. We have already mentioned earlier that the batch form is typically slow in operation due to the computational complexity when $N \gg 1$. Therefore, we proceed with the derivation of a fast iterative form for (20) using recursions in the following.

A. Recursions for General UFIR Filter

In order to derive a fast computation algorithm, we introduce $\bar{\mathbf{x}}_n = \mathbf{S}_{m,n}^{(N)} \mathbf{U}_{m,n}$ and $\bar{\mathbf{Y}}_{m,n} = \mathbf{L}_{m,n}\mathbf{U}_{m,n}$, represent (20) as

$$\hat{\mathbf{x}}_n = \bar{\mathbf{x}}_n + \bar{\mathbf{H}}_{m,n}^h (\mathbf{Y}_{m,n} - \bar{\mathbf{Y}}_{m,n}) \tag{21}$$

and consider the components separately.

1) Homogenous Part: By $\mathbf{u}_n = \mathbf{0}$, the homogenous estimate becomes $\hat{\mathbf{x}}_n = \bar{\mathbf{H}}_{m,n}^h \mathbf{Y}_{m,n}$ and we notice that a fast iterative algorithm for this estimate was proposed in [15]. Given the initial values at $s = n - N + K$ by

$$\mathbf{G}_s = (\tilde{\mathbf{C}}_{m,s}^T \tilde{\mathbf{C}}_{m,s})^{-1} \tag{22}$$

$$\hat{\mathbf{x}}_s = \mathbf{G}_s \tilde{\mathbf{C}}_{m,s}^T \mathbf{Y}_{m,s} \tag{23}$$

where K is the number of the system states and $\mathbf{G}_n$ is the generalized noise power gain, the homogenous UFIR estimate appears iteratively, as shown in [15] to be

$$\mathbf{G}_l = \left[\mathbf{H}_l^T \mathbf{H}_l + (\mathbf{F}_l \mathbf{G}_{l-1} \mathbf{F}^T)^{-1} \right]^{-1} \tag{24}$$

$$\mathbf{K}_l = \mathbf{G}_l \mathbf{H}_l^T \tag{25}$$

$$\hat{\mathbf{x}}_l = \mathbf{F}_l \hat{\mathbf{x}}_{l-1} + \mathbf{K}_l (\mathbf{y}_l - \mathbf{H}_l \mathbf{F}_l \hat{\mathbf{x}}_{l-1}) \tag{26}$$

where an auxiliary variable l ranges from $m + K$ to n and the output is taken when $l = n$.

As can be seen, (26) is the Kalman-like estimate where the bias correction gain $\mathbf{K}_l$ is not the Kalman gain. With each new time step l, the components in $\mathbf{K}_l$ become smaller that improves noise reduction. On the other hand, the bias error grows with l owing to system noise. A compromising value of l minimizes the mse by N_{opt}.

2) Recursion for $\bar{\mathbf{x}}_n$: By formal transformations, we represent $\bar{\mathbf{x}}_n$ recursively as

$$\begin{aligned}
\bar{\mathbf{x}}_n &= \mathbf{S}_{m,n}^{(N)} \mathbf{U}_{m,n} \\
&= \sum_{i=0}^{N-1} \mathcal{F}_n^{n+1-i} \mathbf{E}_{n-i} \mathbf{u}_{n-i} \\
&= \mathbf{E}_n \mathbf{u}_n + \mathbf{F}_n \sum_{i=1}^{N-1} \mathcal{F}_{n-1}^{n+1-i} \mathbf{E}_{n-i} \mathbf{u}_{n-i} \\
&= \mathbf{E}_n \mathbf{u}_n + \mathbf{F}_n \bar{\mathbf{x}}_{n-1}. \tag{27}
\end{aligned}$$

3) Recursions for $\bar{Y}_{m,n} = L_{m,n}U_{m,n}$: In order to find recursions for this component, we rewrite it as

$$\begin{aligned}
\bar{\mathbf{Y}}_{m,n} &= \mathbf{L}_{m,n}\mathbf{U}_{m,n} \\
&= \bar{\mathbf{C}}_{m,n}\mathbf{S}_{m,n}\mathbf{U}_{m,n} \\
&= \bar{\mathbf{C}}_{m,n} \begin{bmatrix} \mathbf{S}_{m,n}^{(1)} \\ \mathbf{S}_{m,n}^{(2)} \\ \vdots \\ \mathbf{S}_{m,n}^{(N-1)} \\ \mathbf{S}_{m,n}^{(N)} \end{bmatrix} \mathbf{U}_{m,n} \tag{28}
\end{aligned}$$

where $\mathbf{S}_{m,n}^{(i)}$, $i \in [1, N]$, is the ith vector row in (6). We then represent the components of $\mathbf{S}_{m,n}\mathbf{U}_{m,n}$ similar to (27) and arrive at

$$\bar{\mathbf{Y}}_{m,n} = \begin{bmatrix} \mathbf{H}_m \mathbf{E}_m \mathbf{u}_m \\ \mathbf{H}_{m+1}(\mathbf{E}_{m+1}\mathbf{u}_{m+1} + \mathbf{F}_{m+1}\bar{\mathbf{x}}_m) \\ \vdots \\ \mathbf{H}_{n-1}(\mathbf{E}_{n-1}\mathbf{u}_{n-1} + \mathbf{F}_{n+1}\bar{\mathbf{x}}_{n-2}) \\ \mathbf{H}_n(\mathbf{E}_n \mathbf{u}_n + \mathbf{F}_n \bar{\mathbf{x}}_{n-1}) \end{bmatrix}. \tag{29}$$

B. Iterative General UFIR Filtering Algorithm

By combining the component $\bar{\mathbf{y}}_l$ of $\bar{\mathbf{Y}}_{m,n}$ with the component $\mathbf{y}_l$ of $\mathbf{Y}_{m,n}$ in (26) and adding (27), we arrive at an estimate

$$\begin{aligned}
\hat{\mathbf{x}}_l &= \mathbf{F}_l \hat{\mathbf{x}}_{l-1} + \mathbf{F}_l \bar{\mathbf{x}}_{l-1} + \mathbf{E}_l \mathbf{u}_l \\
&\quad + \mathbf{K}_l [\mathbf{y}_l - \mathbf{H}_l(\mathbf{F}_l \hat{\mathbf{x}}_{l-1} + \mathbf{F}_l \bar{\mathbf{x}}_{l-1} + \mathbf{E}_l \mathbf{u}_l)] \\
&= \hat{\mathbf{x}}_l^- + \mathbf{K}_l(\mathbf{y}_l - \mathbf{H}_l \hat{\mathbf{x}}_l^-) \tag{30}
\end{aligned}$$

Algorithm 1 General Iterative UFIR Filtering Algorithm

    Data: $\mathbf{y}_n$
    Result: $\hat{\mathbf{x}}_k$
1 **begin**
2   **for** $k = N - 1, N, \cdots$ **do**
3       $m = k - N + 1$, $s = k - N + K$;
4       $\mathbf{G}_s = (\tilde{\mathbf{C}}_{m,s}^T \tilde{\mathbf{C}}_{m,s})^{-1}$;
5       $\tilde{\mathbf{x}}_s = \mathbf{G}_s \tilde{\mathbf{C}}_{m,s}^T (\mathbf{Y}_{m,s} - \mathbf{L}_{m,s}\mathbf{U}_{m,s}) + \mathbf{S}_{m,s}^{(N)}\mathbf{U}_{m,s}$;
6   **for** $l = s + 1 : k$ **do**
7          $\tilde{\mathbf{x}}_l^- = \mathbf{F}_l\tilde{\mathbf{x}}_{l-1} + \mathbf{E}_l\mathbf{u}_l$;
8          $\mathbf{G}_l = [\mathbf{H}_l^T\mathbf{H}_l + (\mathbf{F}_l\mathbf{G}_{l-1}\mathbf{A}_l^T)^{-1}]^{-1}$;
9          $\mathbf{K}_l = \mathbf{G}_l\mathbf{H}_l^T$;
10        $\tilde{\mathbf{x}}_l = \tilde{\mathbf{x}}_l^- + \mathbf{K}_l(\mathbf{y}_l - \mathbf{H}_l\tilde{\mathbf{x}}_l^-)$;
11   **end for**
12       $\hat{\mathbf{x}}_k = \tilde{\mathbf{x}}_k$;
13   **end for**
14 **end**

---

which suggests that the prior estimate is

$$\hat{\mathbf{x}}_l^- = \mathbf{F}_l(\hat{\mathbf{x}}_{l-1} + \bar{\mathbf{x}}_{l-1}) + \mathbf{E}_l\mathbf{u}_l. \tag{31}$$

Now, consider that the estimate at the initial point is supposed to be known. That means that $\bar{\mathbf{x}}_{l-1}$ can be united with $\hat{\mathbf{x}}_{l-1}$ and we finally get

$$\hat{\mathbf{x}}_l = \hat{\mathbf{x}}_l^- + \mathbf{K}_l(\mathbf{y}_l - \mathbf{H}_l\hat{\mathbf{x}}_l^-) \tag{32}$$

where the prior estimate is exactly that of the KF

$$\hat{\mathbf{x}}_l^- = \mathbf{F}_l\hat{\mathbf{x}}_{l-1} + \mathbf{E}_l\mathbf{u}_l. \tag{33}$$

The initial conditions for (33) can be defined at $s = n - N + K$ using a short batch form (20) as

$$\mathbf{G}_s = (\tilde{\mathbf{C}}_{m,s}^T \tilde{\mathbf{C}}_{m,s})^{-1} \tag{34}$$

$$\hat{\mathbf{x}}_s = \mathbf{G}_s\tilde{\mathbf{C}}_{m,s}^T(\mathbf{Y}_{m,s} - \mathbf{L}_{m,s}\mathbf{U}_{m,s}) + \mathbf{S}_{m,s}^{(N)}\mathbf{U}_{m,s} \tag{35}$$

and we finally come up with a general iterative UFIR filtering algorithm which pseudocode is given as Algorithm 1. Two specifics of this algorithm can be indicated in a comparison with the basic iterative UFIR algorithm [15] derived for systems with no inputs. First, like in the KF, the input signal is incorporated here to the prior estimate. Second, the initial state is defined via measurements and input that results in a more complex batch form (35). It is also seen that Algorithm 1 readily simplifies to the basic one for systems with no inputs, by neglecting $\mathbf{u}_l$ and $\mathbf{U}_{m,s}$.

Although the UFIR Algorithm 1 is general and can be applied in line with the KF to any linear problem, we test it by one practical application to GPS-based frequency steering of a local oscillator in the following.

IV. APPLICATIONS

Steering of local oscillators for a reference frequency of a master oscillator is provided when an electronic system operates in a network with synchronized timescales or its operation requires accurate currier. In this section, we use Algorithm 1 to provide GPS-based steering of a local oven-controlled crystal oscillator (OCXO) via measurements of the
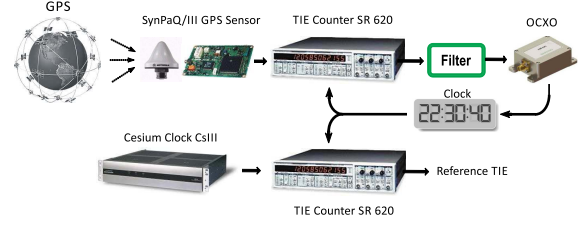

Fig. 1. GPS-based TIE measurement and control set for state estimation and frequency steering in an OCXO-based clock using KF or UFIR filter shown as filter.

time interval error (TIE) using the 1PPS signal available from GPS timing receivers.

A basic structure of the laboratory set used in our experiment[1] is given in Fig. 1. It consists of a GPS SynPaQ III Timing Sensor (Synergy Systems, LLC, San Diego, CA), which receives the 1PPS timing signals from GPS. As a local oscillator, we employ an OCXO imbedded in the Frequency Counter SR620 (Stanford Research System, Inc., Sunnyvale, CA). Another SR620 is used to measure the TIE between the GPS 1PPS signal and a 1 s impulses generated by an OCXO-based local clock. The TIE digital signal measured with a one second time step $\theta = t_n - t_{n-1} = 1$ s goes to an optimal estimator (filter) to estimate the local clock state. The filter output is used to steer the OCXO frequency. To obtain an actual TIE behavior, simultaneous measurements are organized for the reference Cesium Frequency Standard CsIII (Symmetricom, Inc., San Jose, CA), which provides the best available measurements of the TIE. A small frequency offset between the GPS and CsIII frequencies and a time shift between the GPS and CsIII time scales are removed in our set numerically at an early stage by analyzing the TIE on a long baseline.

Note that in view of the precise cost equipment and methods of optimal filtering used in our set, the results presented in the following should be considered as best possible for the implementation in onboard or ground electronic systems.

A. State-Space Model Specification

As stated in [34] and [35], a crystal clock is characterized with three states in the state-space polynomial model. Accordingly, we specify the state vector $\mathbf{x}_n$ in (1) with the TIE x_{1n}, s, fractional frequency offset x_{2n}, and linear fractional frequency drift rate x_{3n}, s^{-1}. In such a model, $\mathbf{x}_{n-1}$ is projected to $\mathbf{x}_n$ with the transition matrix

$$\mathbf{F} = \begin{bmatrix} 1 & \theta & \dfrac{\theta^2}{2} \\ 0 & 1 & \theta \\ 0 & 0 & 1 \end{bmatrix} \tag{36}$$

where $\theta = t_n - t_{n-1}$ is the sampling time. We assign the input signal to be $\mathbf{u}_n = [\, u_{1n} \; u_{2n} \; u_{3n} \,]^T$ with $\mathbf{E}_n$ identity and the clock noise vector as $\mathbf{w}_n = [\, w_{1n} \; w_{2n} \; w_{3n} \,]^T$ with $\mathbf{D}_n$ identity.

---

[1]Measurements were organized and provided by Ing. Luis Arceo-Miquel in the Department of Electronics Engineering of the Universidad de Guanajuato, Salamanca, Mexico.
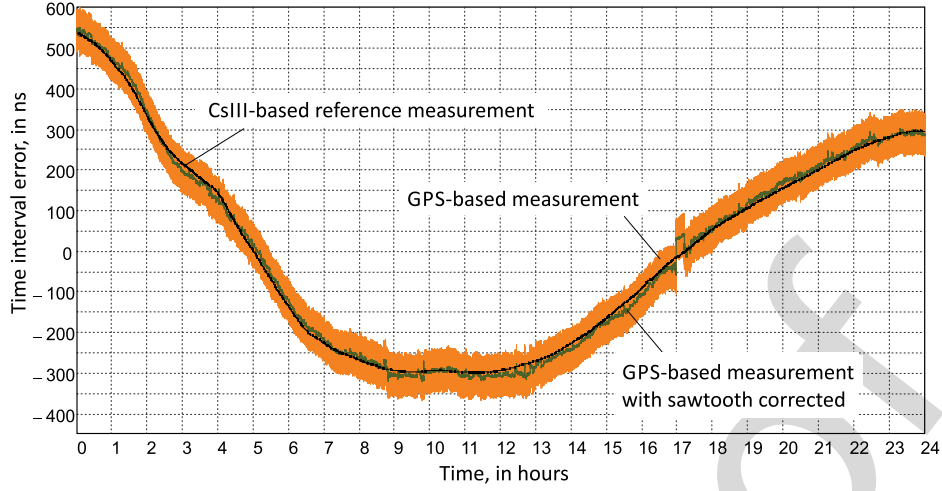
Fig. 2. GPS-based measurements of the TIE (first state) of an OCXO-based clock with sawtooth and sawtooth corrected. Reference measurements are provided using a cesium frequency standard CsIII. The linear trend caused by the difference between the OCXO and GPS frequencies is removed.

Because we measure only the TIE (first state), the observation vector y_n and noise v_n in (2) are both scalar and we project the state vector $\mathbf{x}_n$ onto y_n via $\mathbf{H} = [\,1\ 0\ 0\,]$. Note that the model (36) is also basic for radar tracking of moving objects to estimate the distance, velocity, and acceleration.

1) Tuning KF: To define the clock noise covariance matrix $\mathbf{Q}$, we use the values of the Allan deviation available from the OCXO technical specification in SR620: $\sigma_y(1\ \text{s}) = 2.3 \times 10^{-11}$, $\sigma_y(10\ \text{s}) = 1 \times 10^{-11}$, and $\sigma_y(100\ \text{s}) = 4.2 \times 10^{-11}$. Following [36] and [37], we convert these values into the oscillator diffusion parameters q_1, q_2, and q_3 as:

$$\sigma_y^2(\tau) = \frac{q_1}{\tau} + \frac{q_2\tau}{3} + \frac{q_3\tau^3}{20} \tag{37}$$

where τ is the averaging interval for the Allan deviation. From this relation, we find

$$q_1 \cong 5.29 \times 10^{-4}\ \text{s} \tag{38}$$
$$q_1 \cong 3.00 \times 10^{-9}/\text{s} \tag{39}$$
$$q_1 \cong 3.53 \times 10^{-13}/\text{s}^3 \tag{40}$$

and notice that this model may be inaccurate, because the OCXO noise has nonwhite flicker components that cannot be filtered correctly by the KF. Provided q_1, q_2, and q_3, we refer to [38] and specify the clock covariance matrix as

$$\mathbf{Q} = \theta \begin{bmatrix} q_1 + \dfrac{q_2\theta^2}{3} + \dfrac{q_3\theta^4}{20} & \dfrac{q_2\theta}{2} + \dfrac{q_3\theta^3}{8} & \dfrac{q_3\theta^2}{6} \\ \dfrac{q_2\theta}{2} + \dfrac{q_3\theta^3}{8} & q_2 + \dfrac{q_3\theta^2}{3} & \dfrac{q_3\theta}{2} \\ \dfrac{q_3\theta^2}{6} & \dfrac{q_3\theta}{2} & q_3 \end{bmatrix}. \tag{41}$$

To specify the observation noise covariance, we first notice that the measurement noise induced by the GPS timing receiver is sawtooth and thus not Gaussian. In the commercially available timing sensor SynPaQ III, the sawtooth noise is uniformly distributed from -50 to $+50$ ns and has white properties on a long baseline [10]. We compute the variance

of the sawtooth noise and represent the measurement noise covariance as $R = (50^2/3)$ ns^2. Having no other information, we finally specify the initial clock state with $x_{10} = y_0$, $x_{20} = 0$, and $x_{30} = 0$, and the initial error matrix as $\mathbf{P}_0 = \mathbf{Q}$.

2) Tuning UFIR Filter: Specified $\mathbf{F}_n$ in (1) and $\mathbf{H}_n$ in (2), Algorithm 1 can be used straightforwardly. Faster operation can be achieved if to transform some matrices required to compute the initial values for known $\mathbf{F}$, $\mathbf{H}$, and $\theta = 1$ s as

$$\tilde{\mathbf{C}}_{m,s} = \begin{bmatrix} 1 & -2\theta & 2\theta^2 \\ 1 & -\theta & \dfrac{\theta^2}{2} \\ 1 & 0 & 0 \end{bmatrix}$$

$$\mathbf{G}_s = \begin{bmatrix} 1 & \dfrac{3}{2\theta} & \dfrac{1}{\theta^2} \\ \dfrac{3}{2\theta} & \dfrac{13}{2\theta^2} & \dfrac{6}{\theta^3} \\ \dfrac{1}{\theta^2} & \dfrac{6}{\theta^3} & \dfrac{6}{\theta^4} \end{bmatrix}$$

$$\mathbf{L}_{m,s} = \begin{bmatrix} 1 & 0 & 0 & 0 & 0 & 0 & 0 & 0 & 0 \\ 1 & \theta & \dfrac{\theta^2}{2} & 1 & 0 & 0 & 0 & 0 & 0 \\ 1 & 2\theta & 2\theta^2 & 1 & \theta & \dfrac{\theta^2}{2} & 1 & 0 & 0 \end{bmatrix}$$

$$\mathbf{S}_{m,s}^{(N)} = \begin{bmatrix} 1 & 2\theta & 2\theta^2 & 1 & \theta & \dfrac{\theta^2}{2} & 1 & 0 & 0 \\ 0 & 1 & 2\theta & 0 & 1 & \theta & 0 & 1 & 0 \\ 0 & 0 & 1 & 0 & 0 & 1 & 0 & 0 & 1 \end{bmatrix}.$$

The optimal horizon length of N_{opt} points is a critical characteristic for the UFIR filter. In order to ascertain N_{opt}, we provide test measurements and compute the MSE produced by the UFIR filter for the cesium standard CsIII. We then vary N, minimize the mse, and arrive at $N_{\text{opt}} \cong 3500$. For this horizon, Algorithm 1 consumed about 2.3 s to produce the estimate that was acceptable to discipline frequency each 10 or 100 s. Note that the horizon length can be reduced for acceptable errors, as shown in [39].

Provided the best available parameters for the KF and UFIR filters (Algorithm 1), we notice that the tuning of the UFIR filter by a single N_{opt} is a much simpler way than for the noise statistics and initial values required by the KF. In what follows, we will also show that N_{opt} makes the UFIR filter more accurate than KF in both the clock state estimation and frequency steering.

B. GPS-Based State Estimation of OCXO-Based Clock

We first measure the TIE in the unlocked mode (filter output is not applied to the OCXO) and estimate the clock state. In view of a near constant difference between the OCXO frequency and GPS frequency on a baseline of several hours, the first state x_{1n} as well as its measurements and estimates change almost linearly with hardly recognized deviations. In order to have a more clear picture, we temporary remove a linear trend and show the first state behavior in Fig. 2 on an baseline of 24 h. In Fig. 2, we show the GPS-based measurements, the sawtooth-corrected measurements, and reference measurements provided for the CsIII. Inherently, the GPS-based measurements are accompanied with the zero mean sawtooth noise of ± 50 ns and temporary uncertainties caused by different satellites in a view. Removed the sawtooth, the measurements represent the GPS time uncertainty with a neatly seen excursion in a 15-min span at the 17th hour. Note that this picture varies with time, but not fundamentally, depending on a place and date of measurements in view of the nonstationary orbits of the GPS satellites [10].

We further consider a part of measurements, from 15th to 18th hour, in order to find out how much each estimator is successful in accuracy. The sawtooth noise induced by the receiver is shown in Fig. 3(a) in the presence of the GPS time uncertainty. We obtain it by removing an actual TIE behavior measured using CsIII. Here, we also show the GPS time uncertainty structure obtained by removing the sawtooth.

Fig. 3 exhibits errors which the KF and UFIR filters produce in the estimates of x_{1n} [Fig. 3(b)], x_{2n} [Fig. 3(c)], and x_{3n} [Fig. 3(d)]. Conventionally, we consider all estimates beginning with the first one provided by the UFIR filter on a horizon of $N_{\text{opt}} = 3500$ points. The results confirm a conclusion that was earlier made in [10] and [40]: the UFIR filter is more robust than KF against the GPS time uncertainties and more accurate in clock state estimating. In fact, errors in all of the UFIR estimates (Fig. 3) are more smoothed than those by KF and lie closer to zero. Note that errors in the KF can be reduced by decreasing the $\sigma_y^2(\tau)$ values [40] at $\tau = 1, 10, 100$ s. It, however, turns the Allan variance beyond the OCXO specification. The KF thus does not suit the clock model well and the UFIR definitely is a better choice. This filter outperforms the KF even on a smaller horizon of $N = 1500$. The interested reader can find more results on the clock estimation using UFIR filters in [41]–[44].

C. GPS-Based Steering of OCXO Frequency

Our measurement set is not intended for frequency control that must be organized for each local oscillator
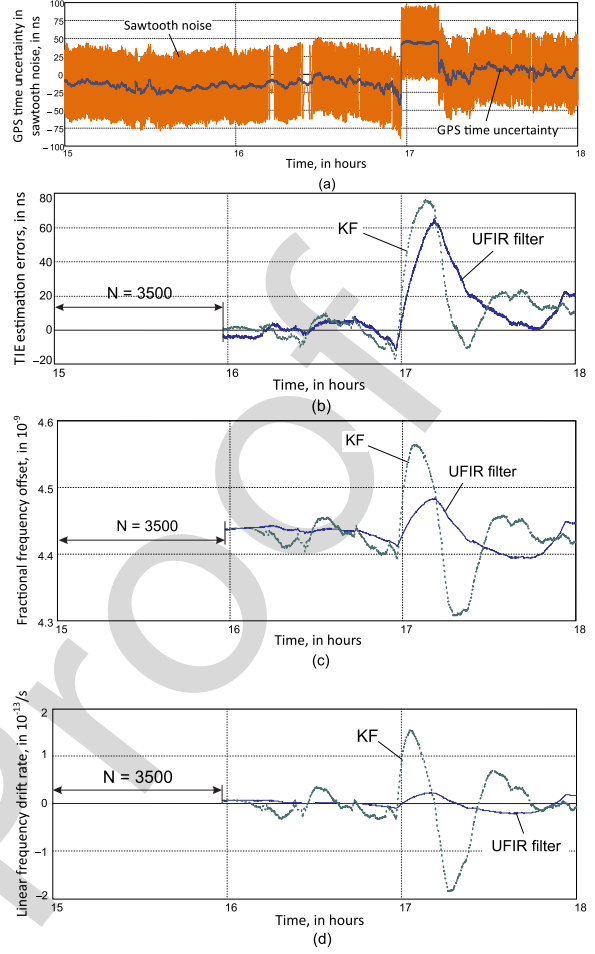

Fig. 3. GPS-based TIE measurements and state estimates of the OCXO-based clock. (a) Sawtooth noise induced by the receiver in the presence of GPS time uncertainty. (b) Errors in the TIE estimates. (c) Fractional frequency offset estimates. (d) Linear frequency drift rate estimates.

individually. Instead, we learn limiting capabilities of OCXO steering by controlling the frequency offset and drift using the KF and UFIR filtering algorithms. We develop it as follows.

Provided the estimate $\hat{\mathbf{x}}_n$ at n, we project it ahead as $\tilde{\mathbf{x}}_{n+1} = \mathbf{F}\hat{\mathbf{x}}_n$ in order to apply to the OCXO at the next time point $n + 1$. We then predict the measurement at $n + 1$ by combining the projected value $\tilde{\mathbf{x}}_{n+1}$ with the sawtooth noise and GPS time uncertainties taken from Fig. 3(a) and united in v_{n+1} to produce

$$\tilde{y}_{n+1} = \mathbf{HF}\hat{\mathbf{x}}_n + v_{n+1}. \tag{42}$$

The OCXO control input is intended to steer the frequency and its drift. Supposing that the control circuit is linearized and normalized in terms of the fractional frequency offset, we organize the feedback by specifying the control signal via estimates. To avoid essential residuals in the OCXO spectrum, we smooth the estimates by simple averaging over $M = 18$ points to have $E\{\hat{x}_{2n}\}_M$ and $E\{\hat{x}_{3n}\}_M$ and assign the
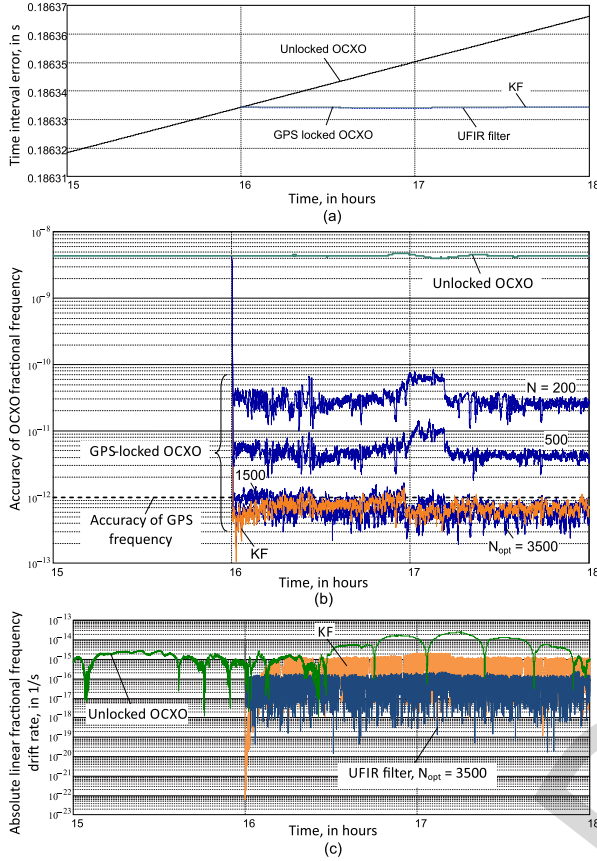
Fig. 4. GPS-based steering of an OCXO using KF and UFIR filters. (a) TIE. (b) Fractional frequency offset. (c) Linear fractional frequency drift rate.

input signal $\mathbf{u}_{n+1}$ as

$$\mathbf{u}_{n+1} = -\mathbf{F} \begin{bmatrix} 0 \\ E\{\hat{x}_{2n}\}_M \\ E\{\hat{x}_{3n}\}_M \end{bmatrix} + \begin{bmatrix} 0 \\ \varepsilon_{n+1} \\ 0 \end{bmatrix} \qquad (43)$$

where ε_{n+1} is a resolution of the digital control circuit. Because the GPS fractional frequency is as accurate as 10^{-12}, we organize steering with a resolution of 10^{-12} and allow the digitization error ε_n to be uniformly distributed from -5×10^{-13} to 5×10^{-13}. We finally include (42) and (43) in Algorithm 1 after line 12 to close the feedback.

The feedback was closed in the algorithms beginning at the 16th hour in order to complete iterations in the UFIR filter and finish transients in the KF. The results of the OCXO frequency steering are shown in Fig. 4. As can be seen [Fig. 4(a)], the clock TIE becomes almost constant after the 16th hour and we notice again that the TIE correction can be provided digitally in the counter. One can also see that both filters correct the TIE function almost equally.

In Fig. 4(b), we demonstrate how accurate each filter is in frequency steering. In the unlocked OCXO, the fractional frequency offset is estimated in average as 4.4×10^{-9} that suits this class of crystal oscillators. On the observed time span, this estimate varied from 4×10^{-9} to 5×10^{-9} due to the GPS time uncertainties. Closed the feedback, both the KF and UFIR filters were successful in reducing the OCXO

frequency offset to the level of 10^{-12} of the GPS reference frequency. But it is also shown in Fig. 4(b) that the UFIR filter produces smaller errors which grow up to the KF errors if to reduce N to $N = 2000$. By $N = 500$, the UFIR guarantees steering with the offset of 10^{-11} and, by $N = 200$, of 10^{-10} that is also acceptable for some applications.

Matrix (36) suggests that the third clock state is constant over time. We, therefore, estimate the OCXO linear fractional frequency drift rate by averaging the available values of of $\hat{x}_{3n}$. In the unlocked mode, x_{3n} was estimated to be of -1.81×10^{-15}/s. In the GPS locking with the KF, it was estimated as 6.29×10^{-17}/s and, with the UFIR filter, as 7.23×10^{-18}/s. These values obtained on a short baseline of several hours can hardly be treated as true. At least, they do not allow us to make any conclusion about the estimator accuracy. We thus further compare the absolute values of the estimates provided by the KF and UFIR filters viewing their envelopes as the estimate bounds. The results are shown in Fig. 4(c). In the unlocked OCXO, the magnitude of $\hat{x}_{3n}$ was estimated by $|\hat{x}_{3n}|$ at a level of 10^{-14}/s. In the locked mode, the KF was successful in reducing the bound to 10^{-15}/s, whereas the UFIR filter reduced it to 10^{-16}/s. Based upon the data shown in Fig. 4(c), one may conclude that the UFIR filter is about 10 times more accurate than the KF in the estimation of the OCXO fractional frequency drift rate. It is not surprising in view of the same conclusion made for the unlocked mode [Fig. 3(d)].

V. CONCLUSION

The general UFIR filter developed in this brief has manifested itself as a robust alternative to the KF. Unlike its basic predecessor, the modified filter can be applied to linear systems with or without control inputs. Its batch form can be used when the computation time is not an issue. Otherwise, we suggest employing the fast Kalman-like iterative algorithm which was developed using recursions. An application to the GPS-based frequency steering of a local OCXO has revealed better robustness and higher accuracy of the general UFIR filter against KF. Both filters were tuned up to their best possible near optimal modes. Nevertheless, the KF filter has demonstrated lower accuracy. Moreover, the determination of a single tuning parameter N_{opt} for the UFIR filter can be provided in a way much simpler than for the noise statistics and initial values required by the KF. We notice it as another advantage of UFIR filtering.

Referring to better engineering features of the proposed UFIR filter, we now focus out attention on other applications related to control problems and adaptive filtering.

REFERENCES

[1] Y. Wang and S. Boyd, "Fast model predictive control using online optimization," *IEEE Trans. Control Syst. Technol.*, vol. 18, no. 2, pp. 267–278, Mar. 2010.

[2] H. L. Van Trees, K. L. Bell, and Z. Tian, *Detection Estimation and Modulation Theory, Part I: Detection, Estimation, and Filtering Theory.* New York, NY, USA: Wiley, 2001.

[3] B. Friedland, "Optimum steady-state position and velocity estimation using noisy sampled position data," *IEEE Trans. Aerosp. Electron. Syst.*, vol. AES-9, no. 6, pp. 906–911, Nov. 1973.

[4] Y. Bar-Shalom, X. R. Li, and T. Kirubarajan, *Estimation With Applications to Tracking and Navigation: Theory Algorithms and Software*. New York, NY, USA: Wiley, 2001.

[5] L. Wang and J. Su, "Robust disturbance rejection control for attitude tracking of an aircraft," *IEEE Trans. Control Syst. Technol.*, vol. 23, no. 6, pp. 2361–2368, Nov. 2015.

[6] A. J. Viterbi and J. K. Omura, *Principles of Digital Communication and Coding*. New York, NY, USA: McGraw-Hill, 1979.

[7] H. G. Berns and R. J. Wilkes, "GPS time synchronization system for K2K," in *Proc. 11th IEEE NPSS Real Time Conf.*, Santa Fe, NM, USA, Jun. 1999, pp. 480–483.

[8] L. Galleani and P. Tavella, "Time and the Kalman filter," *IEEE Control Syst. Mag.*, vol. 30, no. 2, pp. 44–65, Apr. 2010.

[9] "Thunderbolt E GPS disciplined clock, User Guide, Version 1," Trimble, Sunnyvale, CA, USA, Part Number 6405700ENG, Mar. 2012.

[10] Y. S. Shmaliy, *GPS-Based Optimal FIR Filtering of Clock Models*. New York, NY, USA: Nova, 2009.

[11] R. E. Kalman, "A new approach to linear filtering and prediction problems," *J. Basic Eng.*, vol. 82, no. 1, pp. 35–45, Mar. 1960.

[12] M. Partovibakhsh and G. Liu, "An adaptive unscented Kalman filtering approach for online estimation of model parameters and state-of-charge of lithium-ion batteries for autonomous mobile robots," *IEEE Trans. Control Syst. Technol.*, vol. 23, no. 1, pp. 357–363, Jan. 2015.

[13] W. H. Kwon, P. S. Kim, and S. H. Han, "A receding horizon unbiased FIR filter for discrete-time state space models," *Automatica*, vol. 38, no. 3, pp. 545–551, Mar. 2002.

[14] R. J. Fitzgerald, "Divergence of the Kalman filter," *IEEE Trans. Autom. Control*, vol. AC-16, no. 6, pp. 736–747, Dec. 1971.

[15] Y. S. Shmaliy, "An iterative Kalman-like algorithm ignoring noise and initial conditions," *IEEE Trans. Signal Process.*, vol. 59, no. 6, pp. 2465–2473, Jun. 2011.

[16] J. Pomárico-Franquiz, M. Granados-Cruz, and Y. S. Shmaliy, "Self-localization over RFID tag grid excess channels using extended filtering techniques," *IEEE J. Sel. Topics Signal Process.*, vol. 9, no. 2, pp. 229–238, Mar. 2015.

[17] Y. S. Shmaliy, "Linear optimal FIR estimation of discrete time-invariant state-space models," *IEEE Trans. Signal Process.*, vol. 58, no. 6, pp. 3086–3096, Jun. 2010.

[18] A. H. Jazwinski, "Limited memory optimal filtering," *IEEE Trans. Autom. Control*, vol. 13, no. 10, pp. 558–563, Oct. 1968.

[19] A. H. Jazwinski, *Stochastic Processes and Filtering Theory*. New York, NY, USA: Academic, 1970.

[20] W. H. Kwon and S. H. Han, *Receding Horizon Control: Model Predictive Control for State Models*. London, U.K.: Springer, 2005.

[21] O. K. Kwon, W. H. Kwon, and K. S. Lee, "FIR filters and recursive forms for discrete-time state-space models," *Automatica*, vol. 25, no. 5, pp. 715–728, Sep. 1989.

[22] C. K. Ahn, P. Shi, and M. V. Basin, "Two-dimensional dissipative control and filtering for Roesser model," *IEEE Trans. Autom. Control*, vol. 60, no. 7, pp. 1745–1759, Jul. 2015.

[23] C. K. Ahn, L. Wu, and P. Shi, "Stochastic stability analysis for 2-D Roesser systems with multiplicative noise," *Automatica*, vol. 69, pp. 356–363, Jul. 2016.

[24] Y. S. Shmaliy and L. Arceo-Miquel, "Efficient predictive estimator for holdover in GPS-based clock synchronization," *IEEE Trans. Ultrason., Ferroelectr., Freq. Control*, vol. 55, no. 10, pp. 2131–2139, Oct. 2008.

[25] C. K. Ahn, "Strictly passive FIR filtering for state-space models with external disturbance," *Int. J. Electron. Commun.*, vol. 66, no. 11, pp. 944–948, Nov. 2012.

[26] K. V. Ling and K. W. Lim, "Receding horizon recursive state estimation," *IEEE Trans. Autom. Control*, vol. 44, no. 9, pp. 1750–1753, Sep. 1999.

[27] A. M. Bruckstein and T. Kailath, "Recursive limited memory filtering and scattering theory," *IEEE Trans. Inf. Theory*, vol. IT-31, no. 3, pp. 440–443, May 1985.

[28] W. H. Kwon, P. S. Kim, and P. Park, "A receding horizon Kalman FIR filter for discrete time-invariant systems," *IEEE Trans. Autom. Control*, vol. 44, no. 9, pp. 1787–1791, Sep. 1999.

[29] S. H. Han, W. H. Kwon, and P. S. Kim, "Quasi-deadbeat minimax filters for deterministic state–space models," *IEEE Trans. Autom. Control*, vol. 47, no. 11, pp. 1904–1908, Nov. 2002.

[30] S. Zhao, Y. S. Shmaliy, and F. Liu, "Fast computation of discrete optimal FIR estimates in white Gaussian noise," *IEEE Trans. Signal Process. Lett.*, vol. 22, no. 6, pp. 718–722, Jun. 2015.

[31] S. Zhao, Y. S. Shmaliy, and F. Liu, "Fast Kalman-like optimal unbiased FIR filtering with applications," *IEEE Trans. Signal Process.*, vol. 64, no. 9, pp. 2284–2297, May 2016.

[32] H. Stark and J. W. Woods, *Probability, Statistics, and Random Processes for Engineers*, 2nd ed. Upper Saddle River, NJ, USA: Prentice-Hall, 1994.

[33] Y. S. Shmaliy, "Optimal gains of FIR estimators for a class of discrete-time state–space models," *IEEE Signal Process. Lett.*, vol. 15, pp. 517–520, 2008.

[34] *Definitions and Terminology for Synchronization Networks*, document ITU-T Rec. G.810, 1996.

[35] *IEEE Standard Definitions of Physical Quantities for Fundamental Frequency and Time Metrology—Random Instabilities*, IEEE Standard 1139-1999, IEEE, Piscataway, NJ, USA, 1999, pp. 1–36.

[36] R. H. Jones and P. V. Tryon, "Continuous time series models for unequally spaced data applied to modeling atomic clocks," *SIAM J. Sci. Statist. Comput.*, vol. 8, no. 1, pp. 71–81, Jan. 1987.

[37] J. W. Chaffee, "Relating the Allan variance to the diffusion coefficients of a linear stochastic differential equation model for precision oscillators," *IEEE Trans. Ultrason., Ferroelectr., Freq. Control*, vol. UFFC-34, no. 6, pp. 655–658, Nov. 1987.

[38] S. R. Stein and R. L. Filler, "Kalman filter analysis for real time applications of clocks and oscillators," in *Proc. 42nd Annu. Freq. Control Symp.*, Jun. 1988, pp. 447–452.

[39] J. M. Pak, C. K. Ahn, Y. S. Shmaliy, P. Shi, and M. T. Lim, "Switching extensible FIR filter bank for adaptive horizon state estimation with application," *IEEE Trans. Control Syst. Technol.*, vol. 24, no. 3, pp. 1052–1058, May 2016.

[40] J. Contreras-Gonzalez, O. Ibarra-Manzano, and Y. S. Shmaliy, "Clock state estimation with the Kalman-like UFIR algorithm via TIE measurement," *Measurement*, vol. 46, no. 1, pp. 476–483, Jan. 2013.

[41] J. Fu, J. Sun, S. Lu, and Y. Zhang, "Maneuvering target tracking with modified unbiased FIR filter," *J. Beijing Univ. Aeronaut. Astron.*, vol. 41, no. 1, pp. 77–82, Jan. 2015.

[42] Y.-K. Lee, S.-H. Yang, C.-B. Lee, and M.-B. Heo, "Estimation of GPS holdover performance with ladder algorithm used for an UFIR filter," *J. Inst. Control, Robot. Syst.*, vol. 21, no. 7, pp. 669–676, Jul. 2015.

[43] Y. S. Shmaliy and O. Ibarra-Manzano, "Optimal FIR filtering of the clock time errors," *Metrologia*, vol. 45, no. 5, pp. 571–576, Sep. 2008.

[44] Y. Kou, Y. Jiao, D. Xu, M. Zhang, Y. Liu, and X. Li, "Low-cost precise measurement of oscillator frequency instability based on GNSS carrier observation," *Adv. Space Res.*, vol. 51, no. 6, pp. 969–977, Mar. 2013.